Copyright © 2006 Tech Science Press FDMP, vol.2, no.2, pp.127-139, 2006

Three-Dimensional Modeling of the Effects of Misalignment on the Growth of $Ge_{1-x}Si_x$ by The Traveling Solvent Method

M. Sohail[1], **M. Z. Saghir**[1]

Abstract: A numerical simulation study is carried out for the crystal growth of $Ge_{1-x}Si_x$by the Traveling Heater Method (THM). The effects of a geometrical misalignment on the crystal growth are investigated. The full Navier-Stokes equations together with the energy, mass transport and continuity equations are solved numerically using the finite element technique. The application of a misalignment is shown to have a considerable effect on the buoyancy induced flow. An optimal misalignment is determined, that weakens the convective flow, provides a uniform concentration along the growth interface and gives symmetrical characteristics to the three-dimensional buoyancy induced flow.

keyword: Traveling Solvent Method, TSM, Traveling Heater Method, THM, $Si_XGe_{1-X,}$ Misalignment

1 Introduction

The Traveling Solvent Method (TSM) or commonly referred to as the Traveling Heater Method (THM) is a process used to produce pure and homogeneous single crystals that can be used for the production of high quality semiconductors. The TSM process has been tested on many alloys producing uniform and uncontaminated crystal products. It consists of passing a polycrystalline feed rod through a heated solvent zone in order to grow a single crystal by subsequent recrystallization. The solution zone is heated by radiation usually from halogen lamps encompassed in a mirror furnace. The TSM ampoule which contains the crystal, solution zone and the feed rod is translated through the common focus of the furnace's mirrors. Since the TSM process takes place at a lower temperature than other conventional methods (for other crystal growth techniques see, e.g., Lappa, 2005; Gelfgat et al., 2005; Lan and Yeh, 2005; Tsukada et al., 2005, Amberg and Shiomi, etc.), contamination from the container is reduced. The reduced operating temperature also leads to a lower ambient pressure within the growth environment that reduces both the risk of ampoule fracture and the crystal's defect density. Shirakata and Miyake (2003) carried out a study of photo reflectance (PR) measurements on high-quality $CuInS_2$ single crystals grown by the traveling heater method (in which Bulk $CuInS_2$ single crystals were grown from an In solution by THM) and it was found that the crystal quality of the THM-grown $CuInS_2$ was considerable. Yildiz *et al* (2005) studied the liquid phase diffusion (LPD) growth of germanium-rich Si_xGe_{1-x} single crystals by THM and it was found that it is possible to grow good quality Si_xGe_{1-x} single crystals from the germanium-rich side of the Si_XGe_{1-X} by THM.

Wang et al (2005) grew CdZnTe single crystal on CdTe substrate from Te solution with a traveling heater method under a uniform static magnetic induction of 3 T. They pointed out, however, that despite the advantages there are also some disadvantages when growing CdZnTe crystals by the THM, i.e. low thermal conductivity of CdTe makes it difficult to get a stable and flat solid–liquid interface shape during the growth and some other defects such as poly-crystal, twin, boundary and inhomogeneous concentration distribution are often found in the grown crystal. Another disadvantage of THM is its low growth rate, because high growth rates lead to macroscopic defects such as coring and intergranular inclusions in the crystal.

Srivastava et al (2005) studied the influence of the cooling rate of the solution and of the crystal rotation on convection around a growing KDP crystal from its aqueous solution and found that the stable growth regime of the crystal at 0 rpm comprises symmetric buoyancy-generated convection plumes.

Crystal rotation diminishes the concentration gradients, make them more uniform over all faces and improves the symmetry of the concentration distribution in the solution (this leads to a crystal of better quality); the rotation speed of the crystal required to improve crystal quality

[1] Department of Mechanical and Industrial Engineering, Ryerson University, Toronto, On, Canada

depends on the cooling rate of the solution.

Okano et al (2002) carried out a numerical simulation study for the crystal growth of GaSb from a Ga-solution by the THM and investigated the effect of the temperature and crucible rotation on the crystal/solution interface shape. They observed that the use of crucible rotation was very beneficial in suppressing natural convection in the melt and in obtaining an interface with smaller curvature.

In this study the effects of a misalignment (see α in Fig. 1) are considered for the TSM model (with no crystal rotation, i.e. ω=0) under uniform and non- uniform heating conditions, respectively. First the results obtained for the uniform heating condition are discussed, then attention is focused on the non–uniform heating condition.

2 Governing Equations

The three-dimensional steady state Navier-Stokes, energy, mass transport and continuity equations are solved numerically using the finite element technique (Fidap software). The differential equations are as follows:

2.1 Navier-Stokes Equations

r – Component

$$\rho\left[u_r\frac{\partial u_r}{\partial r}+\frac{u_\theta}{r}\frac{\partial u_r}{\partial \theta}-\frac{u_\theta^2}{r}+u_z\frac{\partial u_r}{\partial z}\right]=-\frac{\partial p}{\partial r}+\mu\left[\frac{1}{r}\frac{\partial}{\partial r}\left(r\frac{\partial u_r}{\partial r}\right)+\frac{1}{r^2}\frac{\partial u_r^2}{\partial \theta^2}+\frac{\partial^2 u_r}{\partial z^2}-\frac{u_r}{r^2}-\frac{2}{r^2}\frac{\partial u_\theta}{\partial \theta}\right]-\rho\omega^2 r-2\omega u_r \quad (1)$$

θ – Component

$$\rho\left[u_r\frac{\partial u_\theta}{\partial r}+\frac{u_\theta}{r}\frac{\partial u_\theta}{\partial \theta}+\frac{u_r u_\theta}{r}+u_z\frac{\partial u_\theta}{\partial z}\right]=-\frac{1}{r}\frac{\partial p}{\partial \theta}+\mu\left[\frac{\partial}{\partial r}\left(\frac{1}{r}\frac{\partial}{\partial r}(ru_\theta)\right)+\frac{1}{r^2}\frac{\partial^2 u_\theta}{\partial \theta^2}+\frac{2}{r^2}\frac{\partial u_r}{\partial \theta}+\frac{\partial^2 u_\theta}{\partial z^2}\right] \quad (2)$$

z – Component

$$\rho\left[u_r\frac{\partial u_z}{\partial r}+\frac{u_\theta}{r}\frac{\partial u_z}{\partial \theta}+u_z\frac{\partial u_z}{\partial z}\right]=-\frac{\partial p}{\partial z}+\mu\left[\frac{1}{r}\frac{\partial}{\partial r}\left(r\frac{\partial u_z}{\partial r}\right)+\frac{1}{r^2}\frac{\partial^2 u_z}{\partial \theta^2}+\frac{\partial^2 u_z}{\partial z^2}\right]+\rho g\left[\beta_T(T-T_m)-\beta_c(c-c_0)\right] \quad (3)$$

2.2 Energy Transfer Equation

$$\rho c_p\left[u_r\frac{\partial T}{\partial r}+\frac{u_\theta}{r}\frac{\partial T}{\partial \theta}+u_z\frac{\partial T}{\partial z}\right]=k\left[\frac{1}{r}\frac{\partial}{\partial r}\left(r\frac{\partial T}{\partial r}\right)+\frac{1}{r^2}\frac{\partial^2 T}{\partial \theta^2}+\frac{\partial^2 T}{\partial z^2}\right] \quad (4)$$

2.3 Species Transport Equation

$$u_r\frac{\partial c}{\partial r}+\frac{u_\theta}{r}\frac{\partial c}{\partial \theta}+u_z\frac{\partial c}{\partial z}=-\alpha_c\left[\frac{1}{r}\frac{\partial}{\partial r}\left(r\frac{\partial c}{\partial r}\right)+\frac{1}{r^2}\frac{\partial^2 c}{\partial \theta^2}+\frac{\partial^2 c}{\partial z^2}\right] \quad (5)$$

2.4 Continuity Equation

$$\frac{1}{r}\frac{\partial}{\partial r}(ru_r)+\frac{1}{r}\frac{\partial u_\theta}{\partial \theta}+\frac{\partial u_z}{\partial z}=0 \quad (6)$$

3 Geometrical Model and Boundary Conditions

The TSM model considered here consists of the source material, solvent and germanium single crystal seed where the source rod of $Ge_{0.85}Si_{0.15}$ has a length of 3.6 cm and diameter of 0.8 cm. This rod is positioned on the top of a $Ge_{0.98}Si_{0.02}$ solvent having the same diameter and a length of 1 cm. Both of these components are positioned on germanium single crystal seed. Since silicon has a higher melting temperature than germanium, by having a higher concentration of silicon in the source we are able to keep the solvent in a liquid state while maintaining dissolution interface without any melting. This procedure allows the silicon from the Si-rich source to dissolve slowly through the solvent leading to the diffusion and transport of the silicon to the growth interface for crystallization. Fig. 1(a) shows the geometrical model used in our analysis.

The heater thermal profile used for this simulation was measured experimentally. This temperature profile is shown in Fig. 1(b) and is applied at the external wall of the sample, thereby omitting the quartz tube from our model.

The simulation also incorporates the quasi steady model where the transient effects of heat, mass and fluid flow are considered small enough to be negligible. This approximation is justified due to the slow growth rates typical for the semiconductor materials. Similar approximations have been made by other researchers.

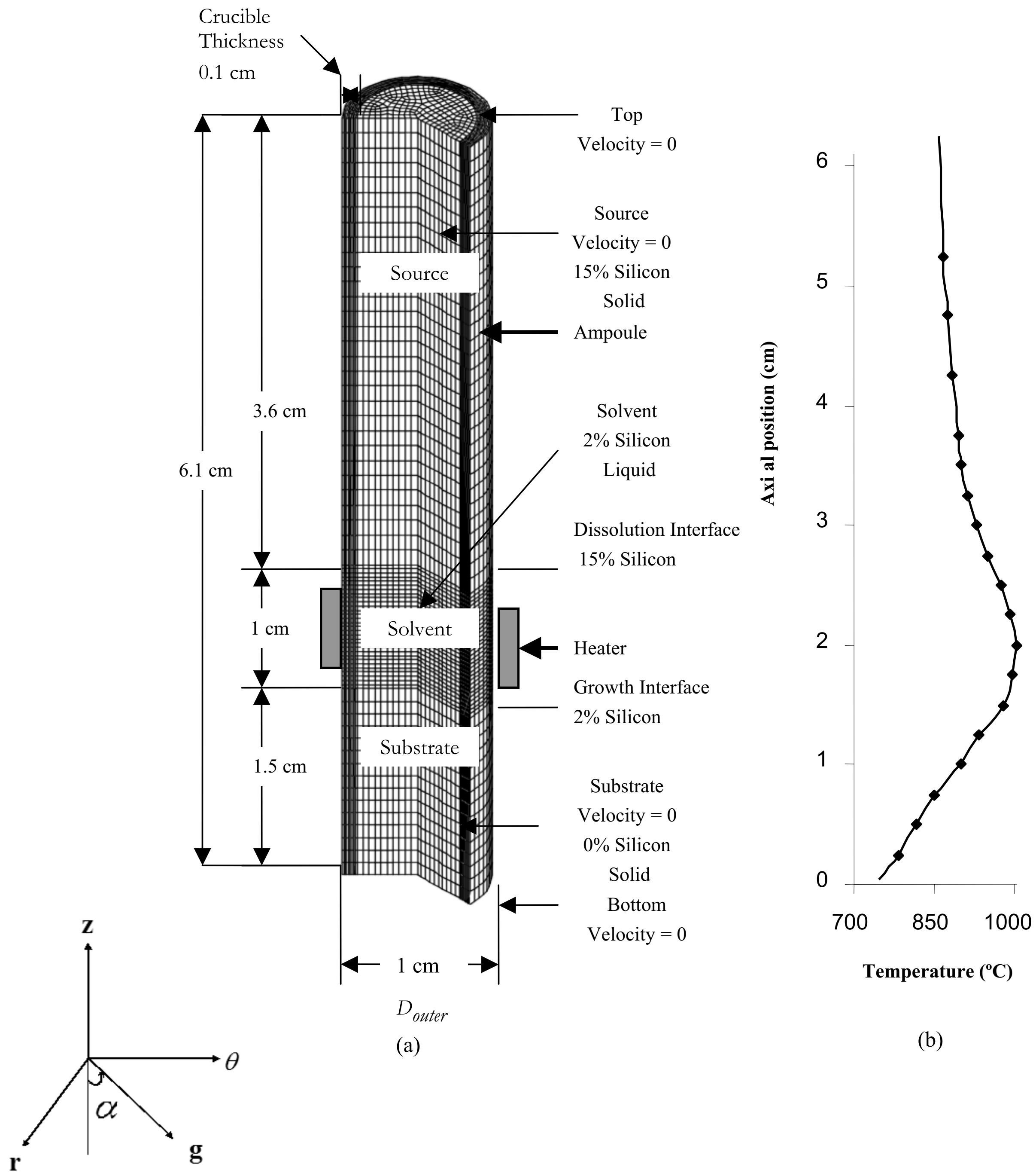

Figure 1 : Model description and boundary conditions: (a) Finite element mesh; (b) Experimentally measured heater thermal profile.

Boundary condition with a zero velocity have been applied to the walls of the crucible and to the liquid/solid interfaces. Only heat diffusion (i.e., V=0) is allowed in the solid (feed rod and crystal) parts.

This model foresees 15 atomic percent of silicon in the source, 2 atomic percent in the solvent, and no silicon in the seed. Accordingly, for the simulation a boundary condition with 15 atomic percent of silicon is applied at the dissolution interface and 2 atomic percent at the growth interface. The application of a concentration

Table 1 : Calculation of the Nusselt numbers for mesh sensitivity

40 Circumferential Elements		**60 Circumferential Elements**	
Axial Elements	**Nusselt Number**	**Axial Elements**	**Nusselt Number**
20	1.669	20	1.649
40	1.546	40	1.540
60	1.492	60	1.518
80	1.478	80	1.470
100	1.460	100	1.446
120	1.451	120	1.441

Table 2 : Source and solvent material properties

Physical Properties of $Ge_{0.98}Si_{0.02}$		**Physical Properties of $Ge_{0.85}Si_{0.15}$**	
Parameter	**Values**	**Parameter**	**Values**
ρ	5.246 g/cm^3	ρ	5.4924 g/cm^3
ν	1.4011x10^{-3} cm^2/s	ν	2.7x10^{-3} cm^2/s
β_c	0.005	β_c	0.005
β_T	1.2x10^{-4}	β_T	1.2x10^{-4}
α_c	1.0x10^{-4} cm^2/s	α_c	2.6x10^{-4} cm^2/s
T_m	971 ^{o}C	T_m	1100 ^{o}C
κ	0.511 W/cm·k	α_T	1.2x10^{-1} cm^2/s
c_p	0.0486 J/g·k	μ	7.35x10^{-3} g/cm·s

value at the growth interface is adopted from Liu et al (2003) and the value is obtained from the Ge-Si phase diagram in Olesinsiki and Abbaschian (1984).

4 Mesh Sensitivity Analysis

Mesh Sensitivity has been carried out for this model in order to ensure accuracy and save computational time. 40 and 30 elements have been used in the axial direction for source and the seed zones, respectively. A finer mesh is not needed in the solid regions. Since the full Navier Stokes, energy transfer and mass transport equations are solved in the solvent, the mesh sensitivity is focused on the solvent part only. The mesh in the solvent zone was varied from 20 to 120 elements in the axial direction in an increment of 20. This was considered for two configurations, one containing 40 circumferential elements and the other 60 circumferential elements. Tab. 1 lists the 12 different solvent meshes considered. The Nusselt numbers calculated for each case are listed in Table 1. It is noted that deviation of the Nusselt number starts to decrease at 80 axial elements and no changes were noticed when reaching 100 and 120 axial elements. According to these results, 100 axial elements with a circumference of 60 elements have been adopted for the numerical grid in the solvent region. The mesh used is constructed of eight node quadrilateral elements having temperature, velocities and pressure as unknowns at each node. When setting up the problem, care was provided when specifying the allowable errors for the solution convergence. An allowance that was too large would result in false convergence, and one that is too small would result in either a very lengthy calculation time, or no convergence at all. The two main error parameters that the finite element program takes into consideration are the velocity convergence tolerance, and the residual vector convergence tolerance. The velocity convergence tolerance is defined by the equation:

$$\left\|\frac{\zeta_i-\zeta_{i-1}}{\zeta_i}\right\| \leq \zeta_{error} \tag{7}$$

where $\zeta$is the solution velocity vector. The error for this case was specified as1×10^{-3}. The residual error on the other hand is defined as:

$$\left\|\frac{R_i}{R_0}\right\| \leq R_{error} \tag{8}$$

The error for this case was also specified to be1×10^{-3}. The norm $\|\|$ is a root mean square norm.

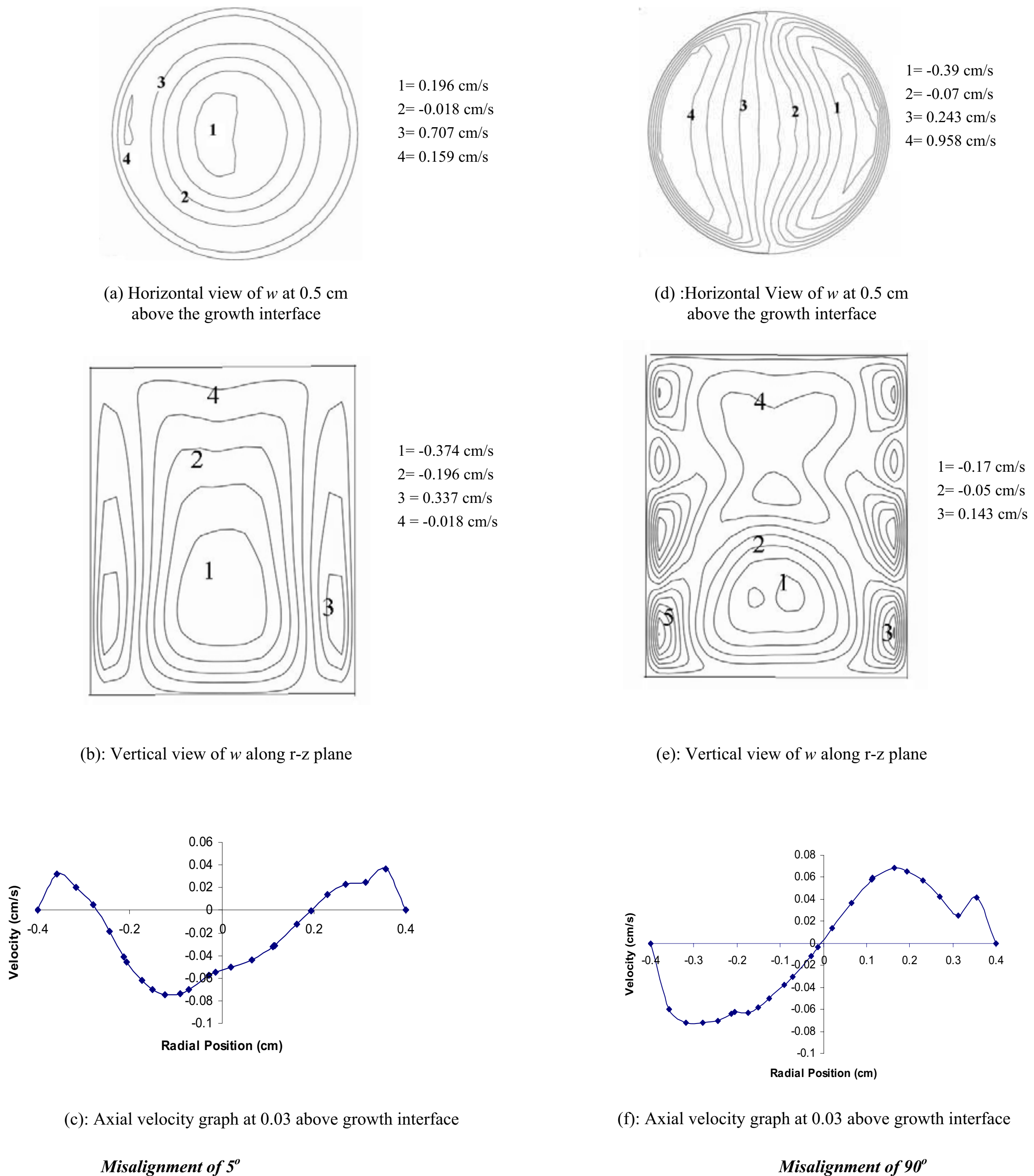

(a) Horizontal view of *w* at 0.5 cm above the growth interface

(b): Vertical view of *w* along r-z plane

(c): Axial velocity graph at 0.03 above growth interface

Misalignment of 5°

(d) :Horizontal View of *w* at 0.5 cm above the growth interface

(e): Vertical view of *w* along r-z plane

(f): Axial velocity graph at 0.03 above growth interface

Misalignment of 90°

Figure 2 : Axial and speed velocity contours (Uniform heating)

5 Results and Discussion:

In this study, misalignment has been applied to the TSM model under uniform and non- uniform heating conditions. The results obtained from the uniform heating condition will be discussed first followed by the non – uniform heating condition.

5.1 Uniform Heating

In the uniform heating condition misalignments of 5°,10°, $45^o$and 90° have been applied to the TSM crystal growth system. The results of the speed contours (w) for

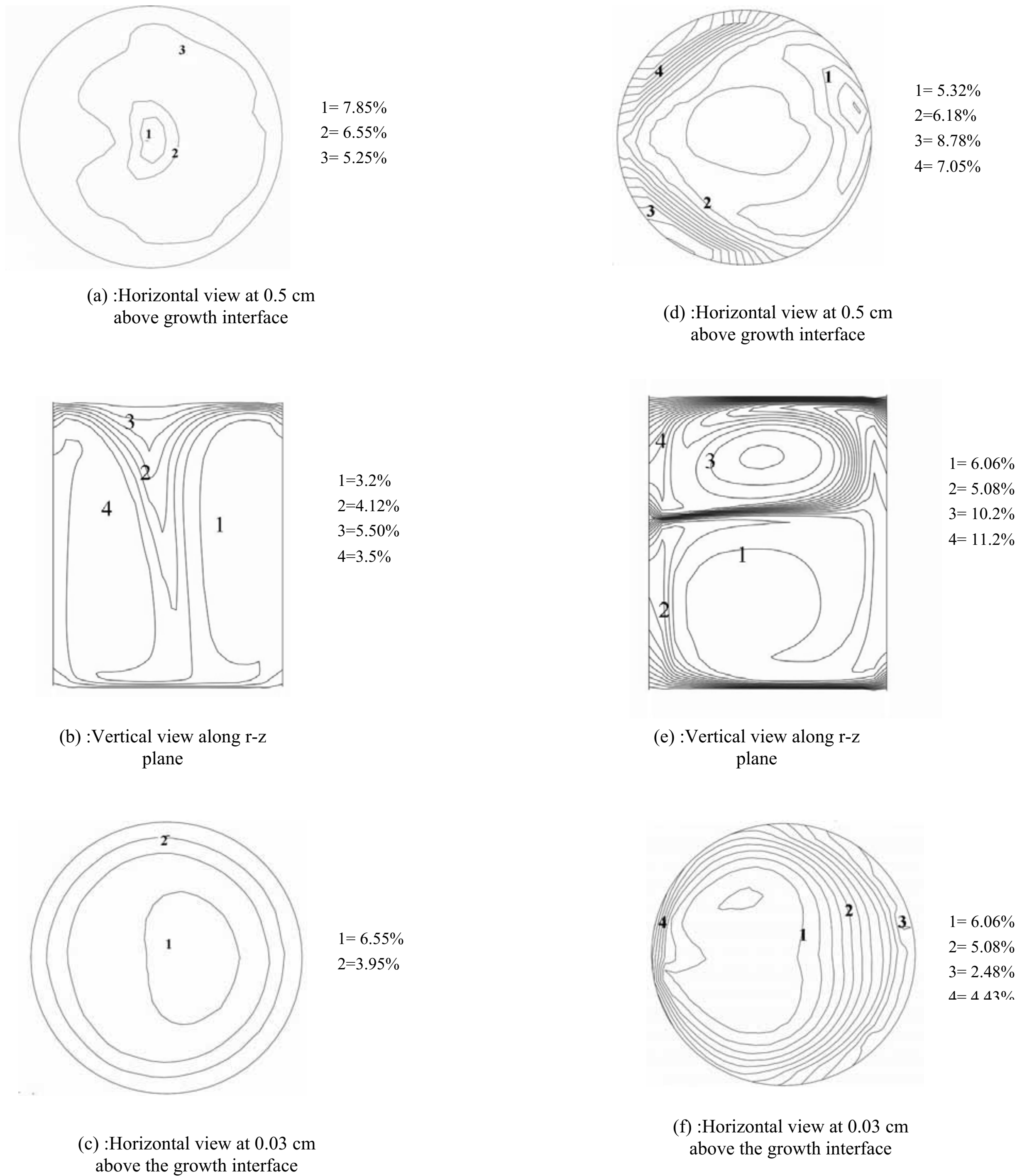

Figure 3 : Silicon distribution contours in the radial and axial direction (Uniform heating)

misalignments of 5° and 90° are shown in Fig. 2. A vertical and a horizontal cut of the solvent and the axial velocity variation along the growth interface are presented. The vertical view shown is that exhibiting the largest evidence of flow dissymmetry. The horizontal view is related to the mid-plane of the solvent zone where the con-

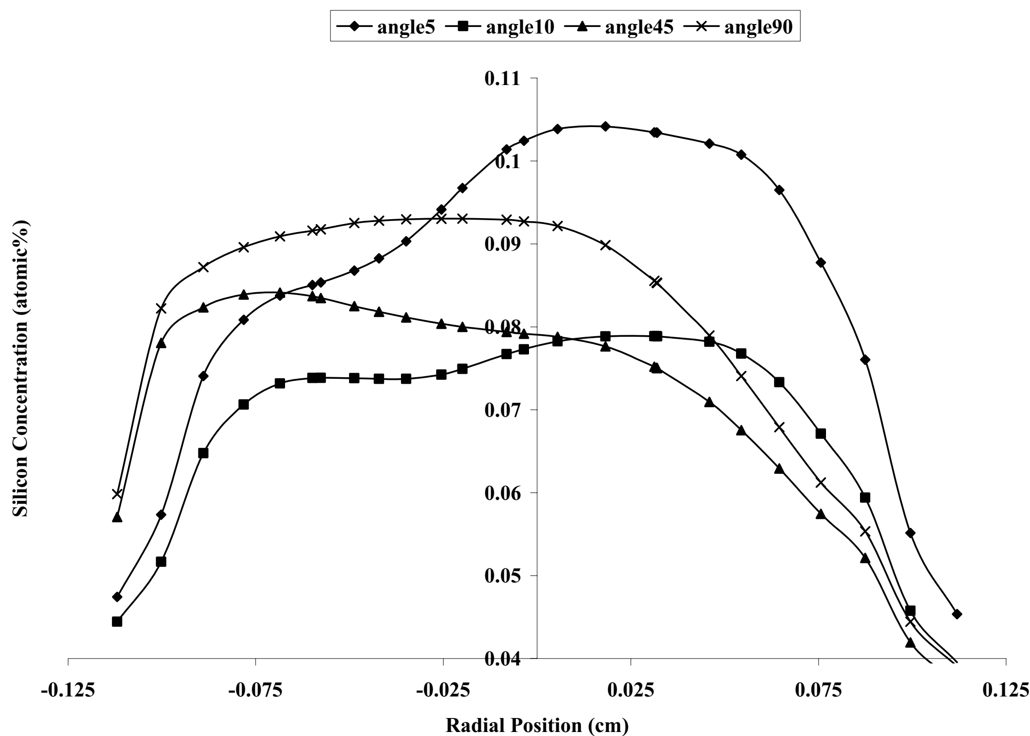

Figure 4 : Silicon distribution contours at 0.03 cm above the growth interface (Uniform heating)

vective current is relatively the strongest.

In the horizontally cut plane (see Figure 2(a)) for the misalignment of 5°, an asymmetry near the centre can be observed .This asymmetry is the result of a three-dimensional characteristic flow within the solution. In the vertical plane as shown in Fig. 2(b) it can be observed that three contour cells have been formed. Here we can see that the highest velocity occurs in the centre of middle contours i.e.-0.374 cm/s negative sign shows that the direction of velocity is downwards, whereas the velocity of 0.337 cm/s is observed at the right side flow cells which shows that the direction is upwards. In Fig. 2(c) where an axial velocity graph at 0.03 cm above the growth interface is shown a noticeable variation from 0.03 cm/s to -0.075cm/s in axial velocity can be observed.

In the horizontally cut plane for the misalignment of 90^oat 0.5 cm above the growth interface (see Fig. 2(d)) two flow cells can be seen where the right side shows the negative velocities which illustrates that the direction of velocity is downwards in the figure whereas the left flow cells show positive velocities which illustrates that the direction is upwards. In the vertical view, as shown in Fig. 2(e), different velocity contours can be observed. Figure 2(f) shows an axial velocity graph which illustrates the variation of velocity from 0.055 cm/s to -0.075 cm/s.

The silicon concentration contours are discussed in Figure 3 where the vertical planes shown are r-z meridian planes and the horizontally cut planes is at 0.5 cm and 0.03 cm above the growth interface. The planes where asymmetry in the silicon distribution is the strongest ate chosen.

In the horizontally cut plane at 0.5 cm above the growth interface for the misalignment of 5° (as shown in Fig. 3(a)) it is evident that concentration contours are asymmetrical as it is proven by the sudden drop of concentration from 7.85% at the centre to 5.25% in the outer contour ring. This is due to the three dimensional characteristic of the flow. In the vertical view, as shown in Fig. 3(b), the highest concentration can be observed along the centre axis of the solvent zone; however, close to the growth interface it becomes lower. This shows that the silicon diffuses down through the centre of the solution zone and then spreads to the sides as it nears the growth interface. In the horizontally cut plane, at 0.03 cm above the growth interface the horizontally cut plane (see Fig. 3(c)) the concentration observed at the centre is 6.55% which drops down to 3.95% near the wall.

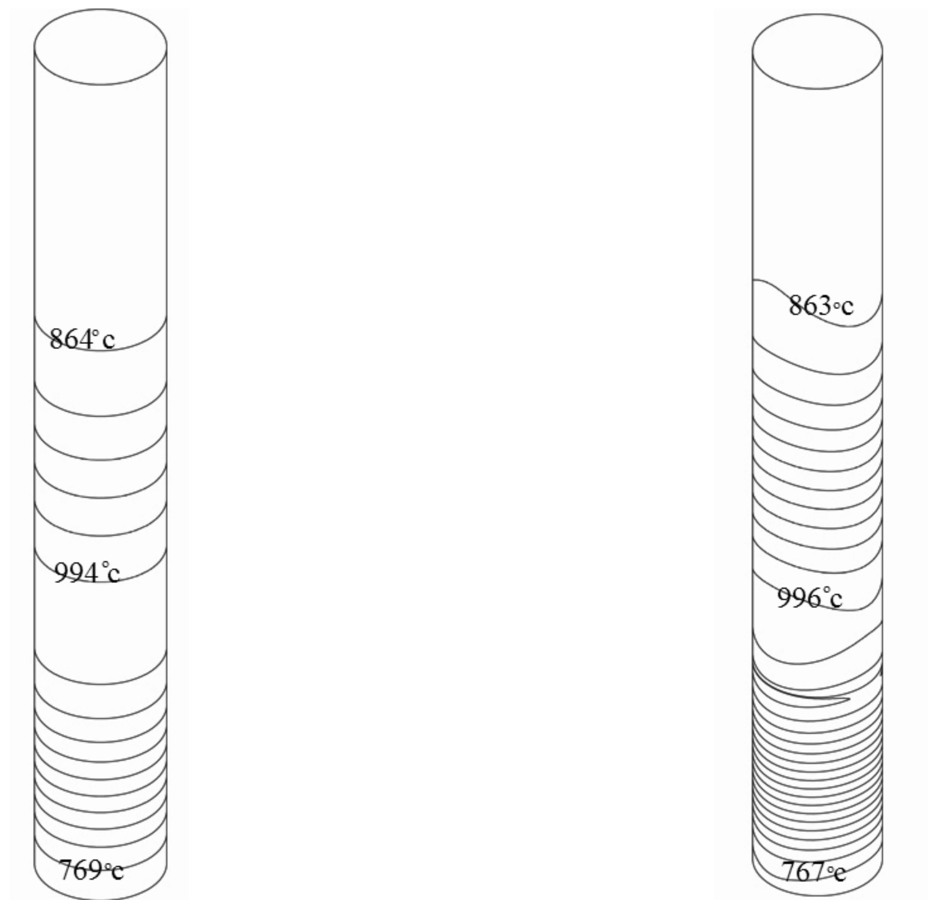

(a) Uniform temperature heater profile

(b) Non-uniform temperature heater profile

Figure 5 : Temperature heating profile for the uniform and non- uniform conditions

The horizontally cut plane at 0.5 cm above the growth interface for the misalignment of 90°,as shown in Fig. 3(d), illustrates that the concentration increases to 7.05%. Fig. 3(e) shows the vertical view. The higher concentration occurs in the upper contour and drops down in the lower contour near the growth interface. This indicates that the direction of flow is from the upper to the lower contour i.e. from dissolution to growth interface. At 0.03 cm above the growth interface the horizontal view (see Fig. 3(f)) shows concentration of 6.06% close to the centre which lessens to 4.43% near the wall.

The silicon concentration distribution graph at 0.03cm above the growth interface for the misalignment of 5°, 10°, 45° and 90° can be seen in Fig. 4. With the misalignment of 5° a non uniform curve is observed with the highest concentration. When the misalignment increases to 10° the concentration drops but a small degree of symmetry can be observed. By increasing the misalignment further to 45° the concentration increases compared to 10^obut the curve obtained is still not very uniform and finally for the misalignment of 90° a more uniform curve is observed. For crystal growth, it is desirable to have a smooth concentration distribution along the growth interface. So for the condition of uniform heating $90^o$is found to be an optimum condition for the crystal growth of $Ge_{1-x}Si_x$.

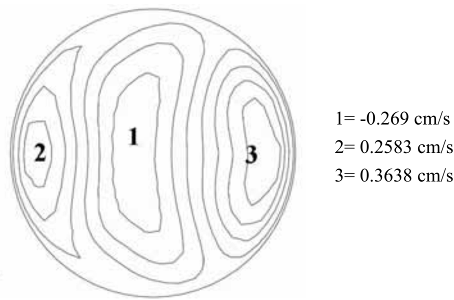

(a) :Horizontal view of *w* at 0.5 cm above growth interface

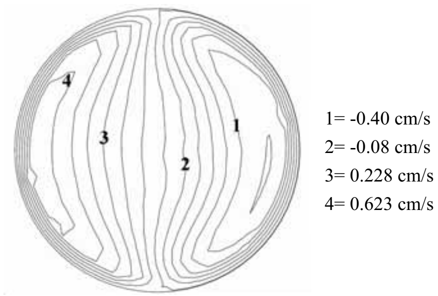

(d) :Horizontal view of *w* at 0.5 cm above the growth interface

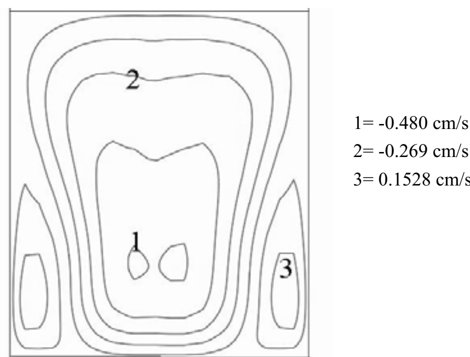

(b) :Vertical view of *w* along r-z plane

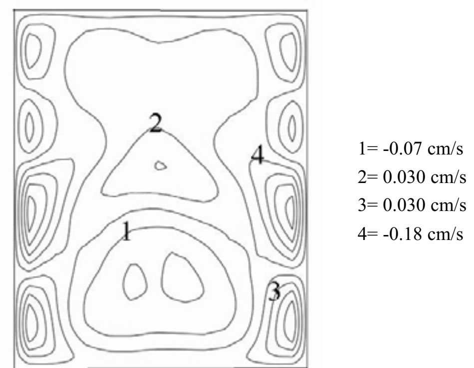

(e) :Vertical view of *w* along r-z plane

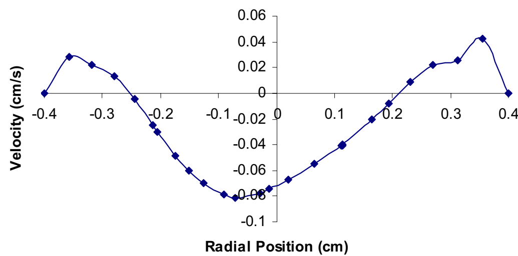

(c) :Axial velocity graph at 0.03 cm above growth interface

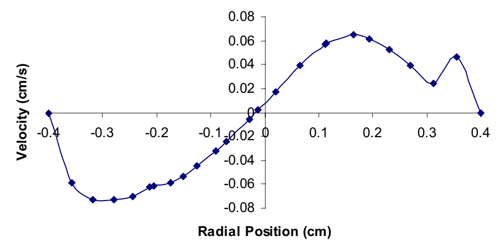

(f) :Axial velocity graph at 0.03 cm above growth interface

Misalignment of 5°

Misalignment of 90°

Figure 6 : Axial and speed velocity Contours (Non- uniform heating)

5.2 Non-Uniform Heating

A non–uniform heater profile has been considered due to the fact that there is practically no heater profile that is uniform. This non-uniform heater profile was obtained by adding a polynomial temperature variation in the x and y directions to the temperature profile applied in the uniform heating conditions. Figure 5 shows the temperature distribution applied for the uniform and non uniform heating conditions.

Figures 6 show a vertical view of the solvent cut in the

1=8.71%
2= 7.85%
3= 4.38%

(a) Horizontal view at 0.5 cm above the growth interface

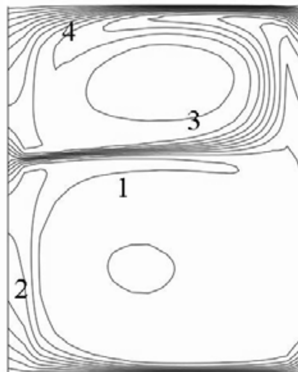

1= 6.983%
2= 14.78%
3= 5.250%

(b) : Vertical view along r-z plane

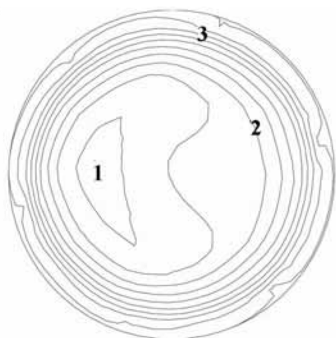

1= 7.850%
2= 6.117%
3= 3.517%

(c) Horizontal view at 0.03 cm above the growth interface

Misalignment of 5°

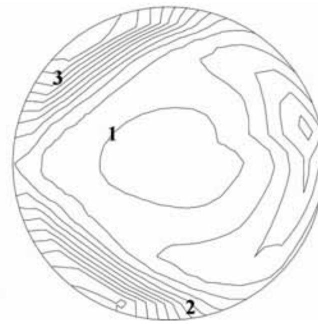

1= 6.06%
2= 7.07%
3= 8.66%

(d) Horizontal view at 0.5 cm above the growth interface

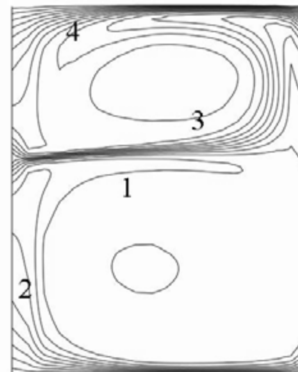

1= 5.90%
2= 4.86%
3= 9.54%
4= 10.4%

(e) : Vertical view along r-z plane

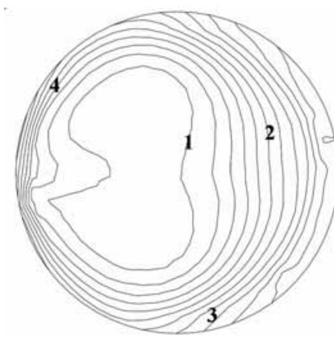

1= 6.06%
2= 5.08%
3= 3.46%
4= 4.43%

(f) Horizontal view at 0.03 cm above the growth interface

Misalignment of 90°

Figure 7 : Silicon distribution contours in the radial and axial direction (Non-uniform Heating)

r-z plane, a horizontally cut plane mid-way through the solvent with two surface graphs and a graph of the axial velocity at 0.03 cm above the growth interface. The r-z plane and the horizontal view mid-plane have been chosen for the same reasoning mentioned previously.

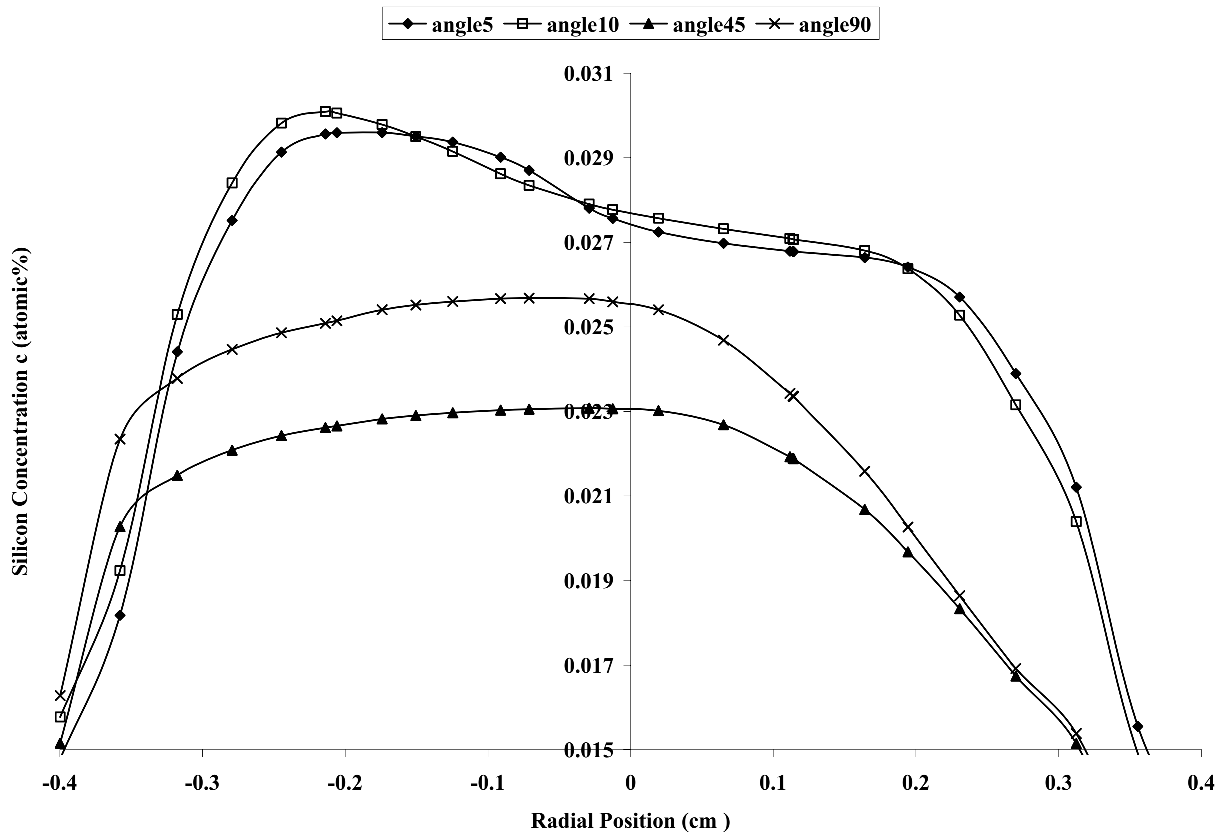

Figure 8 : Silicon distribution at 0.03 cm above the growth interface (Non-uniform heating)

In the horizontally cut plane for the misalignment of 5^oas shown in Figure 6(a) it can be seen that the three contour cells have been formed. The symmetry which was seen in uniform heating has disappeared. In the middle contour cell, velocity of -0.269 cm/s is observed. The negative sign shows that the flow is moving downwards whereas the flow cells at the left and right hand sides show positive velocities of 0.363 cm/s and 0.258 cm/s respectively which shows that the flow is moving upwards. Looking at the vertically cut plane, as shown in Fig. 6 (b), it can be seen that the highest velocity of -0.480 cm/s is observed at the middle contour cell. It is higher than the uniform heating case but the negative sign illustrates that the flow moves downward. The axial velocity plot, as shown in Figure 6(c), illustrates a large variation in flow velocity from 0.025 cm/s to -0.08 cm/s.

In the horizontally cut plane for the misalignment of 90° ,as shown in Figure 6(d), two contour cells can be noticed, where the left flow cell shows negative velocities which elucidates that the flow is moving downward in the figure whereas the positive velocities at the right side show that the flow is moving upwards. In Fig. 6(e) where the vertical view is shown several contour cells of different velocities can be observed. Fig. 6(f) shows the axial velocity graph where the velocity variation from 0.065 cm/s to -0.075 cm/s can be observed.

Fig.7 shows the silicon distribution contours for the misalignments of 5° and 90°. Looking at the horizontal plane cut at 0.5 cm above the growth interface for the misalignment of 5^oas shown in Fig.7 (a) a large jump in silicon concentration can be observed from 8.71% in the centre to 4.38% towards the outer contour ring. Looking at the vertical view (see Fig.7 (b)) it can be seen that the highest concentration of silicon exists along the central axis of the solvent zone, and closer to the growth interface the silicon concentration lessens. This shows that the silicon is diffusing downwards. In the horizontally cut plane at the position of 0.03 cm above the growth interface, as seen in Fig.7(c), the concentration of silicon is observed to be 7.85% at the centre and 3.51% towards the side. This is a large variation of concentration undesirable for crystal growth.

For the misalignment of 90° in the horizontally cut plane at 0.5 cm above the growth interface, as shown in Fig.7(d), concentration increases to 8.66%. In the vertical view, as shown in Fig. 7(e), two contours of different concentration can be observed. The upper contour shows a higher concentration that drops down near the growth interface. This shows that the direction of concentration is from higher to lower concentration. In the horizontally cut plane at 0.03 cm above the growth interface, as seen in Fig. 7(f),concentration at the centre is found to be 6.06% and near the wall it decreases to 4.43%.

Fig. 8 shows the silicon concentration distribution at 0.03 cm above the growth interface for the misalignment of 5°,10°,$45^o$and 90°. With the misalignment of 5° a concave shape is observed which is quite non – uniform whereas for misalignment of 10° it appears that the concentration slightly increases but the curve obtained is still asymmetrical . Now for misalignment of 45° the concentration decreases noticeablely but a small degree of symmetry is observed. Finally, the curve obtained for the misalignment of 90° shows that the concentration further increases. It is evident from the graph that the misalignment of 90° is the most favourable condition in the case of non – uniform heating.

6 Conclusion

A study of buoyancy driven convection in the $Ge_{1-x}\,Si_x$ solution has been conducted under uniform and non- uniform conditions for different misalignments, in order to study the effect of misalignments on the crystal growth by the Traveling Solvent Method. The addition of the misalignment without rotation has been found to suppress buoyancy induced flow throughout the system. For the conditions of uniform and non- uniform heating with no rotational speed the misalignment of 90 ^{o}is the most favorable condition for crystal growth.

Acknowledgement: The authors acknowledge the financial support of the Natural Science and Engineering Council (NSERC).

Nomenclature

c_p : specific heat at constant pressure (J/g·K)
g : gravity (cm/s^2)
Nu $= hl/\kappa$
p : pressure (g/cm^3)
r : radial direction (cm)
T : temperature (K)
u_r : radial velocity (cm/s)
u_z : axial velocity (cm/s)
u_θ : angular velocity (rad/s)
w : speed $\sqrt{u_r^2+u_\theta^2+u_z^2}$ (cm/s)
z : axial direction (cm)

Greek Symbols

α : angle of misalignment
α_c : solutal diffusivity of the species (cm^2/s)
θ : rotation angle about the z-axis
κ : thermal conductivity (W/cm·K)
μ : viscosity (g/cm·s)
ρ : density (g/cm^3)

Subscripts

m : melt

References

Amberg, G.; Shiomi, J. (2005) : Thermocapillary flow and phase change in some widespread materials processes. *FDMP: Fluid Dyn. & Mater. Proc.*, Vol. 1, pp. 81-95.

Edwards.K; Brandon.S; Derby.J. (1999): Transient Effects during the Horizontal Bridgman Growth of Cadmium Zinc Telluride. *J. Crystal Growth*, vol.206, pp. 37-50.

FIDAP. (2002) ,*User Manual*, **8.01**.

Gelfgat A.Yu., Rubinov A., Bar-Yoseph P.Z. and Solan A., (2005): On the Three-Dimensional Instability of Thermocapillary Convection in Arbitrarily Heated Floating Zones in Microgravity Environment , *FDMP: Fluid Dyn. & Mater. Proc.*, Vol. 1, No.1, pp 21-32

Kuppurao.S; Brandon.S ; Derby.J. (1995): Modeling the Vertical Bridgman Growth of Cadmium Zinc Telluride I. Quasi Steady Analysis of Heat Transfer and Convection. *J. Crystal Growth*, vol.155, pp 93-102.

Lan C. W., Yeh B.C., (2005): Effects of rotation on heat flow, segregation, and zone shape in a small-scale floating-zone silicon growth under axial and transversal magnetic fields, *FDMP: Fluid Dyn. & Mater. Proc.*, Vol. 1, No. 1, pp. 33-44.

Lappa M., (2005): Review: Possible strategies for the control and stabilization of Marangoni flow in laterally heated floating zones, *FDMP: Fluid Dyn. & Mater. Proc.*, Vol. 1, No.2, pp. 171-188.

Liu.Y; Dost.S; Lent.B; Redden.F.R. (2003): A Three-Dimensional Numerical Simulation Model for the Growth of CdTe Single Crystals by the Traveling Heater Method under Magnetic Field *.J. Crystal Growth*, vol. 254, pp. 285-297.

Martinez-Tomas.M.C; Munoz-Sanjose.V; Reig.C. (2002): A Numerical Study of Thermal Conditions in the THM Growth of HgTe. *J. Crystal Growth*, vol 243, pp. 463-475.

Okano.Y; Nishino.S; Ohkubo.S; S. Dost.S. (2002): Numerical study of transport phenomena in theTHM growth of compound semiconductor crystal. *J. Crystal Growth*, vol. 237-239, pp .1779-1784.

Olesinski.R.W; Abbaschian.G.J. (1984)**:**. *Alloy Phase Diagrams5*, 180.

Shirakata.S; Miyake. H. (2003): Photo reflectance of $CuInS_2$ single crystal prepared by traveling heater method. *J. Crystal Growth*, vol. 64, pp. 2021-2024.

Srivastava.A; Muralidharand.K; Panigrahi.P.K. (2005):Schlieren study of the effect of ramp rate and rotation on convection around a crystal growing from an aqueous solution. *.J. Crystal Growth, vol.274*, pp. 191-208

Tsukada T., Kobayashi M., Jing C.J. and Imaishi N., (2005): Numerical simulation of CZ crystal growth of oxide, *FDMP: Fluid Dyn. & Mater. Proc.*, Vol. 1, No.1, pp. 45-62.

Wang.Y; Kudo.K; Y. Inatomi; Motegi.T. (2005): Growth and structure of CdZnTe crystal from Te solution with THM technique under static magnetic field**.** *J. Crystal Growth,* vol. 275, pp. 1551-1556

Ye.X; Tabarrok.B; Walsh.D. (1996): Influence of Thermal Solutal Convection on CdTe Growth by the Traveling Heater Method. *Journal of Crystal Growth*, vol.169, pp. 704-714.

Yildiz, M; Dostand.S; Lent.B. (2005): Growth of bulk SiGe single crystals by liquid phase diffusion.*.J. Crystal Growth*, vol. 280, pp. 151-160.